Supporting information for

A Neutral Porous Organic Polymer Host for the Recognition of Anionic Dyes in Water

Whitney S. Y. Ong[a], Ronald A. Smaldone*[,a], and Sheel C. Dodani*[,a]

[a]Department of Chemistry and Biochemistry, The University of Texas at Dallas, 800 West Campbell Road, Richardson, TX 75080

*Email: sheel.dodani@utdallas.edu, ronald.smaldone@utdallas.edu

Experimental

General synthetic materials and methods. Reagents and chemicals were purchased from Alfa Aesar, Electron Microscopy Sciences, Matrix Scientific, Oakwood Chemicals, Sigma-Aldrich, TCI America, Strem Chemicals, or Thermo Fisher Scientific and were used as received. The syntheses of the starting materials for the porous organic polymers (POPs) are shown in Scheme S1. Representative procedures are described below. All compounds were purified using SiliaFlash Irregular Silica Gel P60 (SiliCycle) or with preloaded cartridges on a CombiFlash NextGen 300 flash chromatography system (Teledyne ISCO Inc.). NMR spectra were collected at 25 °C on a Bruker AVANCE III HD spectrometer in the Molecular and Protein Analysis Core Facility at The University of Texas at Dallas. Chemical shifts (δ) are reported in parts per million versus the residual proton and carbon signals of the deuterated NMR solvent (Figure S1). High-resolution electrospray ionization mass spectra (HR-ESI-MS) were acquired on a Waters SYNAPT G2-Si mass spectrometer.

1,4-dibromo-2-(bromomethyl)benzene (1a). The synthesis of compound **1a** was adapted from a previously reported procedure for 5-bromo-2-chlorotoluene.[1] A solution of N-bromosuccinimide (7.76 g, 43.6 mmol) in MeCN (150 mL) was purged with a stream of nitrogen for 15 min, followed by the addition of 2,5-dibromotoluene (4 mL, 29.1 mmol) and benzoyl peroxide (1.41 g, 5.81 mmol). The reaction mixture was heated to reflux overnight under a nitrogen atmosphere. The next day, the reaction mixture was cooled to room temperature, quenched with sodium sulfite (*ca.* 1 g), and concentrated *in vacuo*. The crude reaction mixture was dissolved in CH_2Cl_2 (50 mL) and washed with water (3 x 50 mL) and brine (3 x 50 mL). The organics were combined, dried over anhydrous Na_2SO_4, and concentrated *in vacuo*. The resulting crude solid was recrystallized from methanol to furnish a white powder (1.30 g, 45%). The purity was determined with NMR spectroscopy and was consistent with that previously reported.[2]

2-(2,5-dibromobenzyl)isoindoline-1,3-dione (1b). The synthesis of compound **1b** was adapted from a previously reported procedure.[3] Potassium phthalimide (3.59 g, 19.4 mmol) was added to a solution of compound **1a** (4.25 g, 12.9 mmol) in anhydrous DMF (15 mL) under a stream of nitrogen. The reaction mixture continued to stir overnight at room temperature under a nitrogen atmosphere. The next day, the reaction mixture was quenched with water (20 mL), and the resulting precipitate was collected by vacuum filtration, washed with water (50 mL), and dried to yield a white powder (5.06 g, 99%). The purity was determined with NMR spectroscopy and was consistent with that previously reported.[3]

(2,5-dibromophenyl)methanamine (1c). The synthesis of compound **1c** was adapted from a previously reported procedure.[3] Compound **1b** (4.98 g, 12.6 mmol) was dissolved in absolute EtOH (30 mL) at 90 °C under a nitrogen atmosphere. A solution of anhydrous hydrazine (25 mL, 80.3 mmol) was added dropwise to the reaction. The reaction mixture continued to stir for 6 h at reflux under a nitrogen atmosphere. The resulting golden yellow solution was cooled to room temperature, quenched slowly with a saturated solution of $NaHCO_3$, and extracted with CH_2Cl_2 (3 x 20 mL). The organics were combined, washed with water (2 x 50 mL), dried over anhydrous Na_2SO_4, and concentrated *in vacuo* to generate a light yellow solid (2.76 g, 82%). The purity was determined with NMR spectroscopy and was consistent with that previously reported.[3]

[(2,5-dibromophenyl)methyl]urea (1). The synthesis of compound **1** was adapted and modified from a previously reported procedure for the preparation of benzylurea deriviatives.[4] Concentrated HCl (*ca*. 1 mL) was added dropwise to a suspension of compound **1c** (2.00 g, 7.55 mmol) in water. The reaction mixture was heated to 90 °C to dissolve all of the solids.

Potassium isocyanate (0.92 g, 11.32 mmol) in water (5 mL) was added dropwise to the resulting solution, and the reaction mixture continued to stir for 4 h at 90 °C. The reaction mixture was cooled to room temperature, and the resulting precipitate was collected by vacuum filtration, washed with water (100 mL), and dried to yield a white powder (2.15 g, 92%).^{1}H NMR (600 MHz, DMSO-d_6): δ 7.54 (d, J = 8.34 Hz, 2H), 7.41 (s, 1H), 7.39 (d, J = 8.34 Hz, 2H), 6.56 (t, J = 5.82, 5.88 Hz, 1H), 5.72 (s, 2H), 4.17 (d, J = 6.06 Hz, 2H). ^{13}C NMR (150 MHz, DMSO-d_6,): δ 158.53, 142.18, 134.20, 131.28, 130.89, 120.99, 120.86, 43.04. HR-ESI-MS calculated for $[C_8H_8Br_2N_2O + H]^+$ m/z = 306.9076, found m/z = 306.9157.

1,3,5-tris((trimethylsilyl)ethynyl)benzene (3a). The synthesis of compound **3a** was adapted from a previously reported procedure.[5] Triethylamine (9 mL, 57.5 mmol) in a heavy-walled pressure flask was purged with a stream of nitrogen for 20 min, followed by the addition of 1,3,5-tribromobenzene (50 mg, 1.59 mmol), bis(triphenylphosphine)palladium(II) dichloride ($Pd(PPh_3)_2Cl_2$) (33 mg, 0.05 mmol), and copper iodide (CuI) (9.1 mg, 0.05 mmol). The reaction mixture was purged with a stream of nitrogen for an additional 15 min prior to the addition of trimethylsilylacetylene (0.88 mL, 6.35 mmol). Following this, the pressure flask was immediately sealed, and the reaction mixture continued to stir for 16 h at 65 °C. The following day, the reaction mixture was cooled to room temperature, filtered, washed with hexanes (50 mL) on a silica plug, collected, and concentrated *in vacuo*. The resulting residue was purified by flash chromatography (silica, hexanes) to afford a pale-yellow solid (500 mg, 86%). The purity was determined with NMR spectroscopy and was consistent with that previously reported.[6]

1,3,5-triethynylbenzene (3). The synthesis of compound **3** was adapted from a previously reported procedure.[5] A solution of K_2CO_3 (108 mg, 0.78 mmol) in water (0.4 mL) was added to a solution of compound **3a** in a mixture of THF and MeOH (7:2 ratio, 9 mL). The reaction mixture continued to stir for 6 h at room temperature. Water (10 mL) was added to dilute the reaction mixture, and the product was extracted with CH_2Cl_2 (3 x 10 mL). The organics were combined, washed with water (20 mL), dried over anhydrous Na_2SO_4, and concentrated *in vacuo* to furnish an off-white solid (203 mg, 98%). The purity was determined with NMR spectroscopy and was consistent with that previously reported.[6]

Urea-POP-1 (4). A solution of triethylamine (1 mL, 7.17 mmol) and toluene (3 mL, 56.5 mmol) in a heavy-walled pressure tube was purged with a stream nitrogen for 20 min followed by the addition of **1** (154 mg, 0.50 mmol), **3** (50 mg, 0.33 mmol), CuI (13 mg, 0.07 mmol), and tetrakis(triphenylphosphine)palladium ($Pd(PPh_3)_4$) (380 mg, 0.03 mmol). The pressure tube was immediately sealed, and the reaction mixture continued to stir overnight 95 °C. The following day, the reaction mixture was cooled to room temperature, and the resulting solid was filtered and washed sequentially with hexanes (100 mL), CH_2Cl_2 (100 mL), MeOH, 2M HCl (20 mL), water (100 mL), and acetone (100 mL). Impurities from the remaining solid were removed through Soxhlet extractions with THF (2 d) and MeOH (1 d). The resulting solid was collected by filtration to produce Urea-POP-1 as a brown powder (70 mg, 57%).

Methyl-POP-1 (5). Following the procedure described above for Urea-POP-1, 2,5-dibromotoluene (**2**) (0.68 mL, 0.50 mmol) was used in place of compound **1**, and Methyl-POP-1 was isolated as a dark brown powder (75 mg, 82%).

General methods to characterize Urea-POP-1 and Methyl-POP-1. Attenuated total reflectance Fourier transform infrared (ATR-FTIR) spectra of starting materials **1**, **2**, and **3** and finely ground Urea-POP-1 and Methyl-POP-1 were collected at 25 °C on an Agilent Cary 660 FTIR Spectrometer (Agilent) in the Molecular and Protein Analysis Core Facility at The University of Texas at Dallas. Representative FTIR spectra are shown in Figure S2.

The Micromeritics ASAP 2020 Accelerated Surface Area and Porosimetry System (Micromeritics Instrument Corporation) was used to characterize six independently prepared batches of Urea-POP-1 and Methyl-POP-1. Briefly, at least 30 mg of each POP was degassed under dynamic vacuum for 12 h at 120 °C, followed by exposure to nitrogen (up to 760 torr, 99.999%, Airgas Corporation) in a liquid nitrogen bath at 77 K. Based on these nitrogen adsorption isotherms, the surface areas were determined using the Brunauer-Emmett-Teller (BET) model with the data points collected at relative pressures between 0.01 and 0.1 P/P_0. The pore size distributions were determined using the Dubinin-Raduskevich (DR) model and non-localized density functional theory (NLDFT) carbon slit-pore model in the Micromeritics software package. The surface areas are summarized in Table S1, and the nitrogen isotherms and pore size distributions are shown in Figure S3.

Scanning electron microscopy (SEM) was performed on a Zeiss Supra 40 Scanning Electron Microscope (Carl Zeiss Microscopy) in the Cleanroom Research Laboratory at The University of Texas at Dallas. Briefly, the samples were ground into fine powder and transferred onto double-sided copper tape on 15 mm aluminum stubs. The samples were imaged at an approximate working distance of 8 mm with a voltage of 5 kV for Urea-POP-1 and 10 kV for Methyl-POP-1. Representative SEM images for both POPs are shown in Figure S4. Powder X-ray diffraction measurements of both POPs were performed on a Rigaku SmartLab X-ray diffractometer in the Nano Characterization Facility at The University of Texas at Dallas with Cu Kα (1.54060 Å) at 40 kV and 30 mA using a low background sample holder. The data were collected at 0.05° intervals from 2° to 30°. Representative diffraction patterns for both POPs are shown in Figure S4.

Determination of the yields for Urea-POP-1 and Methyl-POP-1. The representative yields of both POPs stated above were determined by dividing the mass of the POP synthesized by the molecular weight of each repeating unit, and then divided by the total molar amounts of the starting materials used. Each repeating unit was defined as the molar ratio of starting materials added into the reaction – two units of **3** and three units of **1** or **2** as shown in Figure S5.

Anionic dye adsorption assays with Urea-POP-1 and Methyl-POP-1. The anionic dyes used were: adenosine 5'-monophosphate sodium salt (AMP), adenosine 5′-triphosphate disodium salt hydrate (ATP), Alizarin Yellow G sodium salt, bromophenol blue sodium salt, riboflavin 5'-monophosphate sodium salt hydrate (FMN), fluorescein disodium salt, Lucifer Yellow CH dilithium salt, methyl orange sodium salt, methyl red sodium salt, and Rhodamine B chloride. Stock solutions of each dye were prepared at 500 μM in ultrapure water (*ca.* pH 7). Stock solutions of each POP were prepared in ultrapure water at 1 mg/mL or 2 mg/mL and sonicated for *ca.* 2 h in an ultrasonic bath (Branson Ultrasonics). For each assay, the dye and POP were combined in a 1.5 mL microcentrifuge tube to a final volume of 500 μL. The dye stock solutions were diluted to a final concentration of 40 μM, and the POP stock solutions were diluted to 0.05, 0.1, 0.2, 0.4, 0.6 and 0.8 mg/mL for the carboxylate and sulfonate dyes and 0.1, 0.2, 0.4, 0.8, 1.2, and 1.6 mg/mL for the phosphonate dyes. After incubation for 30 min at room temperature, each sample was centrifuged for 5 min at 20000*g* at room temperature (5810 R, Eppendorf). For all of the dyes, except AMP and ATP, a 100 μL aliquot of each supernatant was transferred to a 96-well half-area microtiter plate (Greiner Bio-One). Absorbance spectra were collected for all of the dyes on a plate reader (Tecan). However, due to interference in the absorbance spectra for samples with Urea-POP-1, fluorescence spectra were collected for FMN and Lucifer Yellow CH. Plate reader settings for each dye are summarized in Table S2. Due to background interference in the UV region from fine POP particulates, absorbance spectra for AMP and ATP were measured on the Agilent Cary 7000 Universal Measurement Spectrophotometer (Agilent) in the Molecular and Protein Analysis Core Facility at The University of Texas at Dallas. Briefly, the AMP and ATP samples were filtered via centrifugation for 2 min at 2000*g* at room

temperature (5810 R, Eppendorf) through Zymo-Spin I Columns (Zymo Research). The filtered samples were transferred to a 0.2-cm x 1-cm quartz cuvette (0.4 mL, Hellma USA) for measurements. Representative absorbance and emission spectra from different POP batches tested are shown in Figures S6–S15. To determine the percentage of dye adsorbed to each POP (A_f/A_0 or F_f/F_0), the measured absorbance (A_f) or fluorescence (F_f) value of each sample was divided by the absorbance (A_0) or fluorescence (F_0) value of the dye alone at a particular wavelength that was within the linear limit of detection as specified in Table S2. For all of the dyes, except AMP and ATP, both A_f and A_0 was background corrected by subtracting the absorbance of water alone (A_{H2O}) at the wavelength specified in Table S2. For AMP and ATP, this background correction was accounted for in the spectrophotometer software. The fluorescence spectra did not require background correction. For each dye, the average of at least three technical replicates with standard deviation from at least two different batches of each POP is presented in Figure 3. This was done to account for variability in particle size, pore size distribution, and surface area of each POP batch.

Determination of the amount of Urea-POP-1 at a 95% saturation point. The saturation point at 95% was defined as where the relative absorbance or fluorescence signal of each dye had less than a 5% change. These saturation points were then used to calculate the amount of Urea-POP-1. A representation of this is shown in Figure 4A. The saturation points were determined by plotting the absorbance $A = [A_{obs} - A_{min}]/[A_{max} - A_{min}]$ or fluorescence $F = [F_{obs} - F_{min}]/[F_{max} - F_{min}]$ ratio versus the concentration of Urea-POP-1 from Figure 3 in KaleidaGraph v4.5 (Synergy Software). A_{obs} or F_{obs} is the observed absorbance or fluorescence value of the supernatant in the presence of Urea-POP-1, A_{max} or F_{max} corresponds to the absorbance or fluorescence value of the initial dye concentration in the absence of Urea-POP-1, and A_{min} or F_{min} corresponds to the absorbance or fluorescence value of the dye in the presence of the maximum concentration of Urea-POP-1 used. For each dye, at least three individual datasets were fitted to the following equation A or F = 1 – (m1*[Urea-POP-1]) / (m2 + [Urea-POP-1] to determine the m1 and m2 constants. These constants were then used to calculate the amount of Urea-POP-1 at the 95% saturation points where A or F = 0.05. The average of at least three technical replicates with standard deviation from at least two different batches of each POP is presented in Figure S16 and Table S3.

Determination of partition coefficients. A previously reported procedure was adapted to measure the partition coefficients or log *D* values of each dye.[7] Each dye was prepared at 40 or 50 μM in ultrapure water (*ca.* pH 7). Equal volumes of each dye solution in water (750 μL) and octanol (750 μL) were combined into a 2-mL microcentrifuge tube, mixed for 1 min at maximum speed (Vortex 2 Shaker, IKA Works), and centrifuged for 5 min at 2900*g* at room temperature (5810 R, Eppendorf). For each dye, a 100 μL aliquot of the water layer was transferred to a 96-well half-area microtiter plate, but for AMP and ATP, a 200 μL aliquot of the water layer was transferred to a 96-well UV-Star UV-Transparent microtiter plate (Greiner Bio-One). The absorbance or fluorescence of each dye was measured as described above, compared to a standard curve, and used to determine the log *D* values as follows: $\log D = \log([dye]_{octanol}/[dye]_{water})$ where $[dye]_{water}$ corresponds to the concentration of partitioned dye in water and $[dye]_{octanol}$ corresponds to the concentration of partitioned dye in octanol which was measured through mass balance. The average of three technical replicates with standard deviation is reported in Table S3.

Scheme S1. Synthesis of (A) [(2,5-dibromophenyl)methyl]urea (**1**) and (B) 1,3,5-triethynylbenzene (**3**).

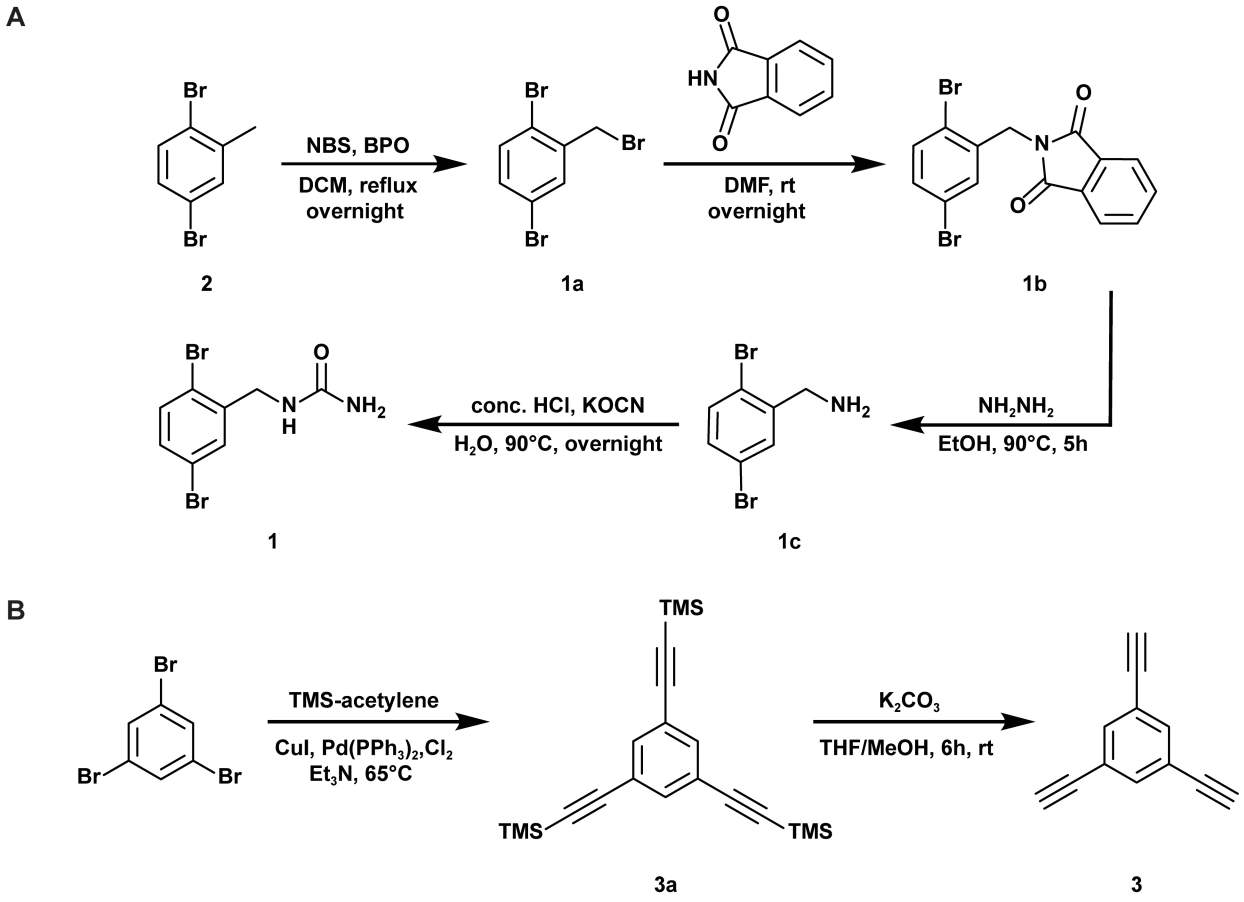

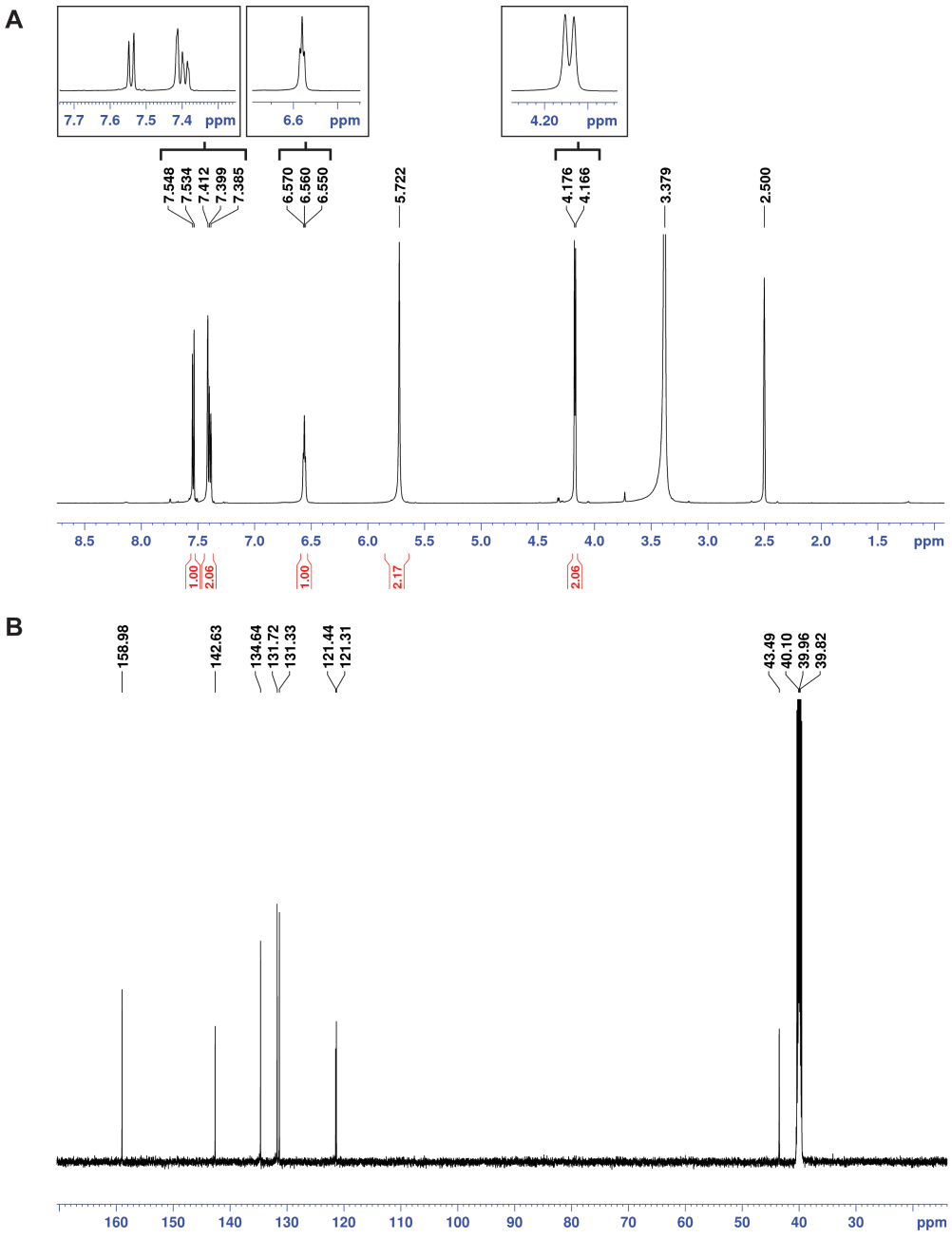

Figure S1. (A)^{1}H-NMR and (B) ^{13}C-NMR spectra of [(2,5-dibromophenyl)methyl]urea (**1**).

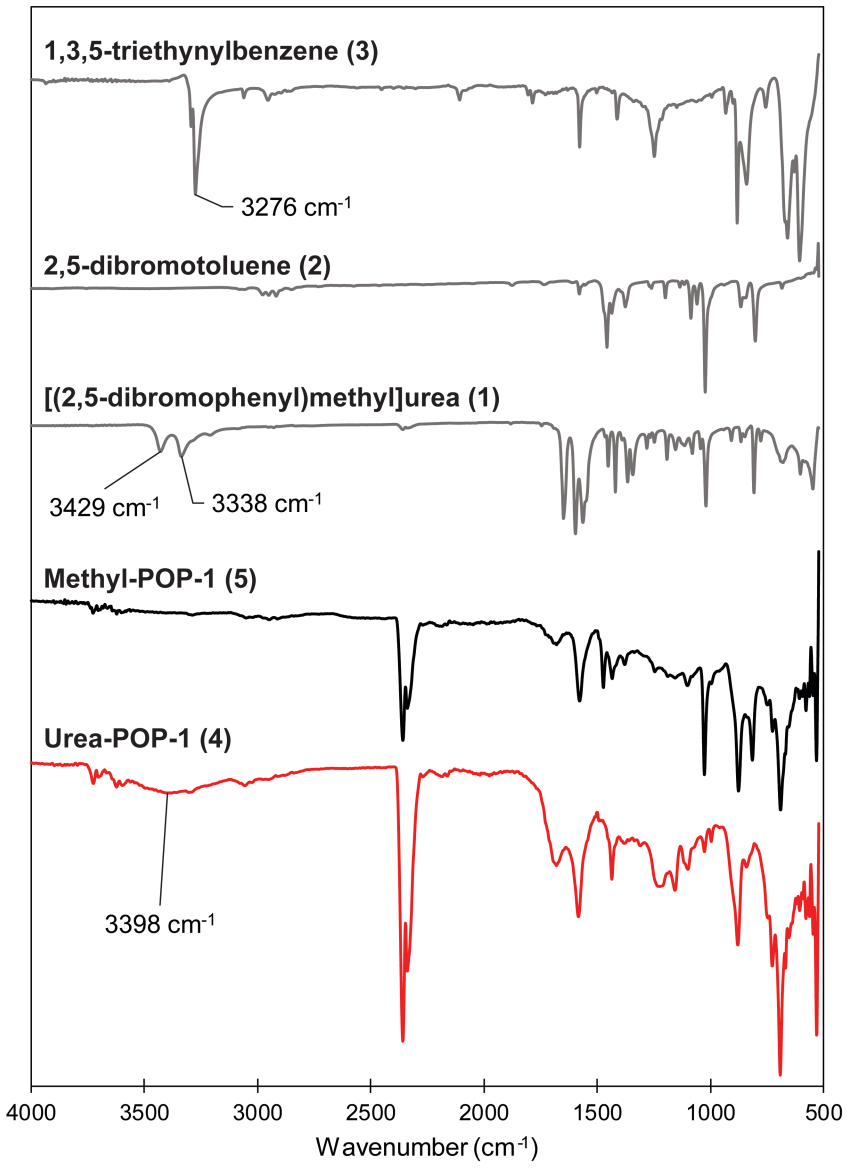

Figure S2. Stacked attenuated total reflectance Fourier transform infrared (ATR-FTIR) spectra of starting monomers and POPs.

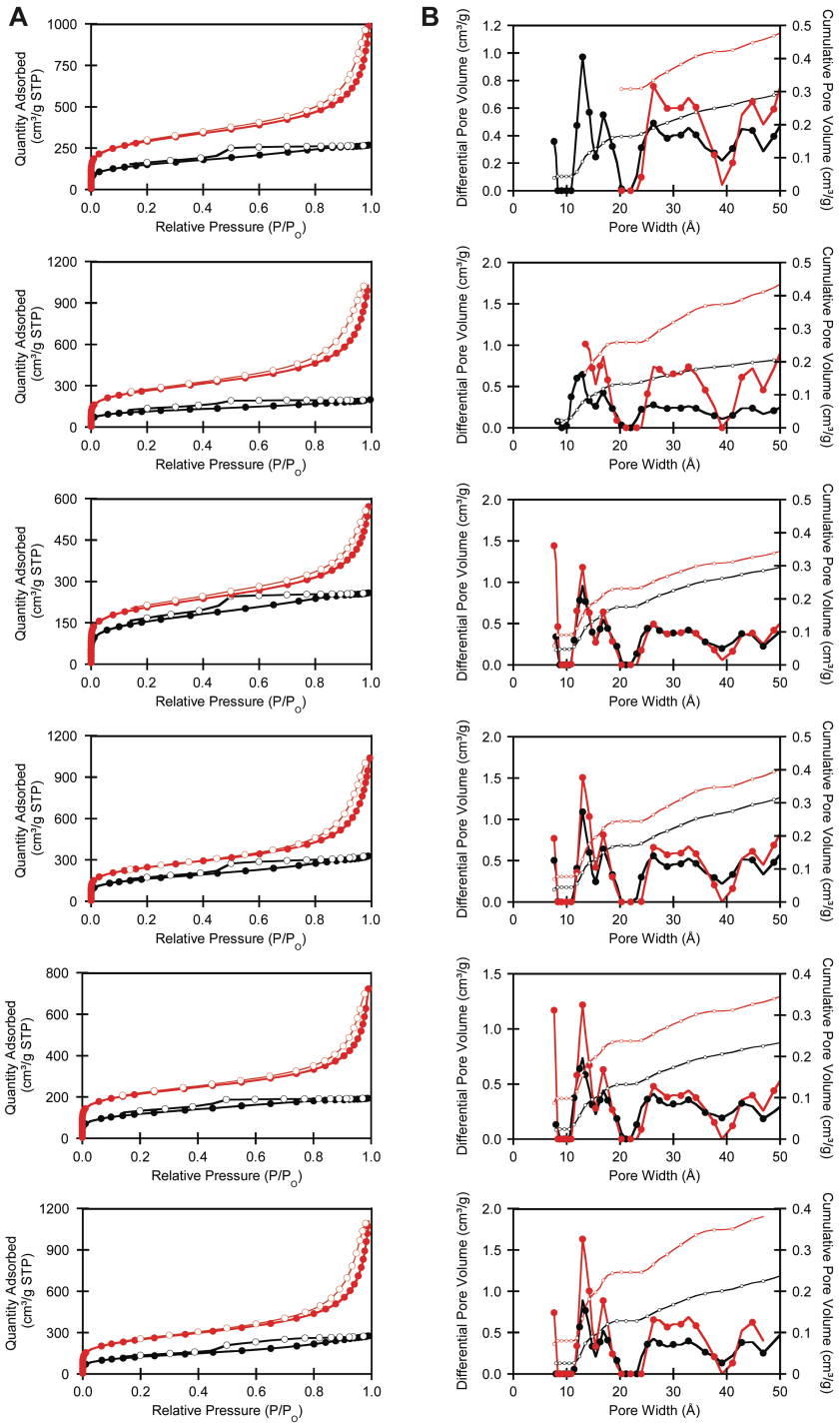

Figure S3. Comparison of the (A) nitrogen adsorption (closed circles) and desorption (open circles) isotherms and (B) differential (closed circles) and cumulative (open circles) pore volumes for Urea-POP-1 (red) and Methyl-POP-1 (black). Data is shown for six independently prepared batches of each POP corresponding to Table S1.

Table S1. BET surface areas for six independently prepared batches of Urea-POP-1 and Methyl-POP-1. The average with standard deviation is reported.

Batch	BET surface areas (m^2/g)						
	1	2	3	4	5	6	Average
Urea-POP-1	1041	936	743	873	718	885	870 ± 120
Methyl-POP-1	530	409	550	572	417	438	490 ± 70

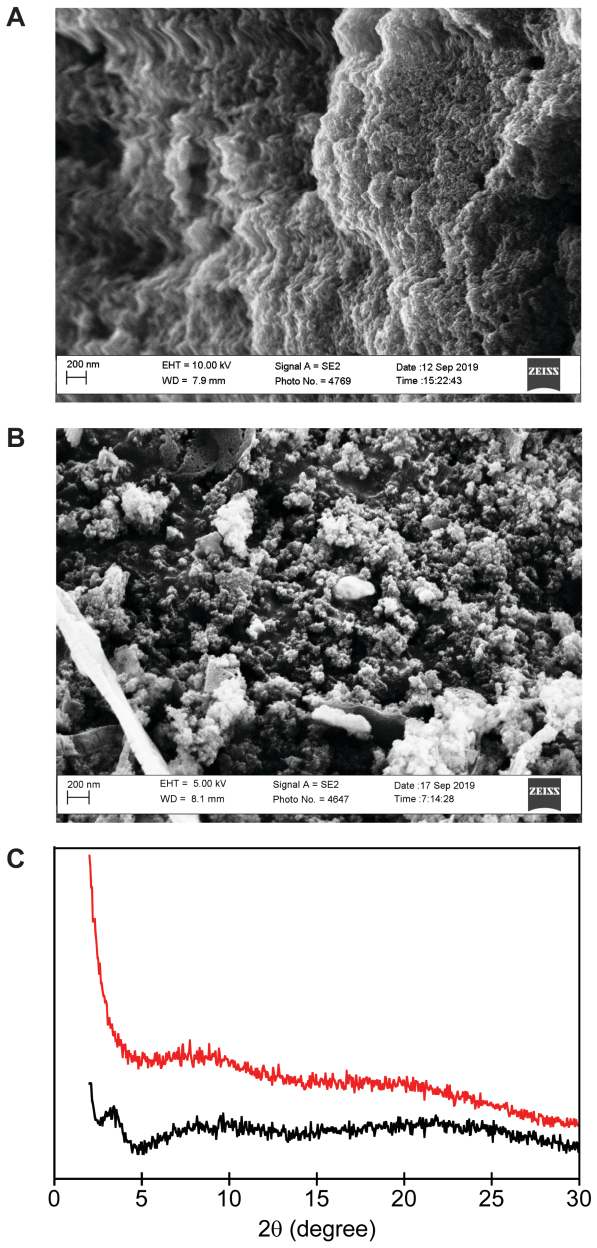

Figure S4. Representative scanning electron microscopy (SEM) images of (A) Urea-POP-1 and (B) Methyl-POP-1 and (C) powder X-ray diffraction patterns of Urea-POP-1 (red) and Methyl-POP-1 (black).

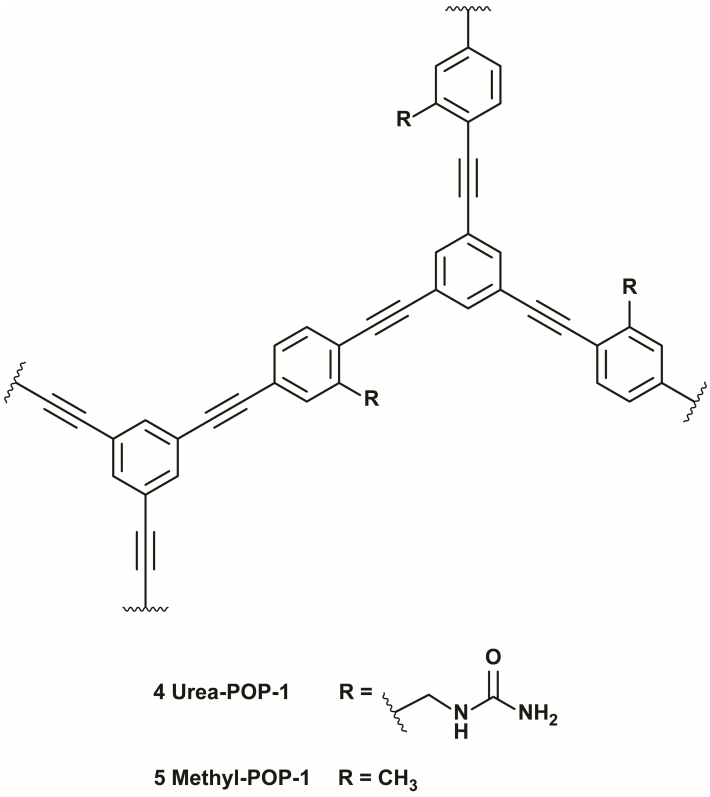

Figure S5. Structure of the monomer unit for Urea-POP-1 (738.80 g/mol) and Methyl-POP-1 (564.68 g/mol).

Table S2. Plate reader settings for each dye.

Dyes	Absorbance[c]		Fluorescence[c]				
	Range (nm)	$\lambda_{measured}$ (nm)	Excitation (nm)	Emission (nm)	$\lambda_{measured}$ (nm)	Flashes	Gain
FMN[a]	300–800	450	450	480–800	530	30	100
AMP[a,b]	230–300	260	N/D	N/D	N/D	N/D	N/D
ATP[a,b]	230–300	260	N/D	N/D	N/D	N/D	N/D
Methyl orange	350–650	465	N/D	N/D	N/D	N/D	N/D
Lucifer Yellow CH	350–700	425	430	450–700	535	30	90
Bromophenol blue	450–700	560	N/D	N/D	N/D	N/D	N/D
Rhodamine B	450–650	530	N/D	N/D	N/D	N/D	N/D
Methyl red	360–560	435	N/D	N/D	N/D	N/D	N/D
Alizarin Yellow G	330–480	350	N/D	N/D	N/D	N/D	N/D
Fluorescein	400–600	475	N/D	N/D	N/D	N/D	N/D

[a] Abbreviations: Flavin mononucleotide (FMN), adenosine monophosphate (AMP), adenosine triphosphate (ATP)
[b] UV-visible spectrophotometer was used instead
[c] Spectra were collected with a 5 nm step size

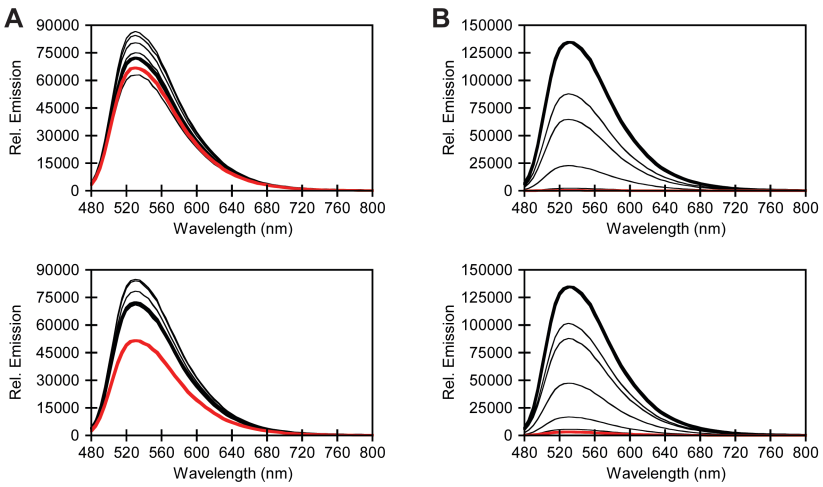

Figure S6. Representative fluorescence spectra of flavin mononucleotide (FMN) in the presence of increasing concentrations of (A) Methyl-POP-1 and (B) Urea-POP-1 for two different batches. The POP concentrations range from 0 (black, bold), 0.1, 0.2, 0.4, 0.8, 1.2 and 1.6 (red) mg/mL. All measurements were carried out with 40 μM of FMN in ultrapure water (*ca.* pH 7).

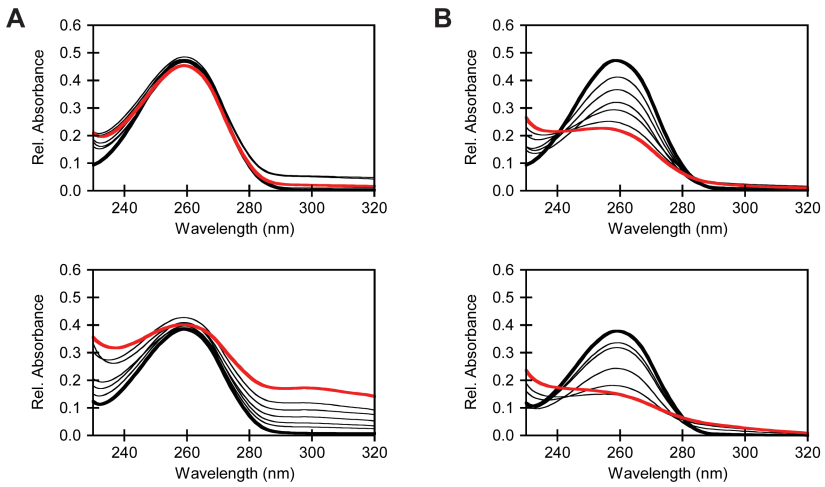

Figure S7. Representative absorbance spectra of adenosine monophosphate (AMP) in the presence of increasing concentrations of (A) Methyl-POP-1 and (B) Urea-POP-1 for two different batches. The POP concentrations range from 0 (black, bold), 0.1, 0.2, 0.4, 0.8, 1.2 and 1.6 (red) mg/mL. All measurements were carried out with 40 µM of AMP in ultrapure water (*ca.* pH 7). Note: With higher concentrations of Methyl-POP-1, interference was observed at longer wavelengths due to light scattering from fine particulates that passed through the filter.

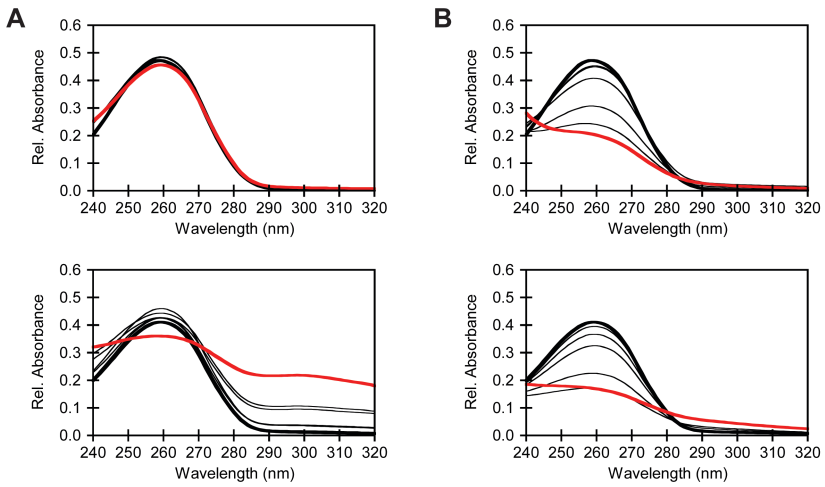

Figure S8. Representative absorbance spectra of adenosine triphosphate (ATP) in the presence of increasing concentrations of (A) Methyl-POP-1 and (B) Urea-POP-1 for two different batches. The POP concentrations range from 0 (black, bold), 0.1, 0.2, 0.4, 0.8, 1.2 and 1.6 (red) mg/mL. All measurements were carried out with 40 µM of ATP in ultrapure water (*ca.* pH 7). Note: With higher concentrations of Methyl-POP-1, interference was observed at longer wavelengths due to light scattering from fine particulates that passed through the filter.

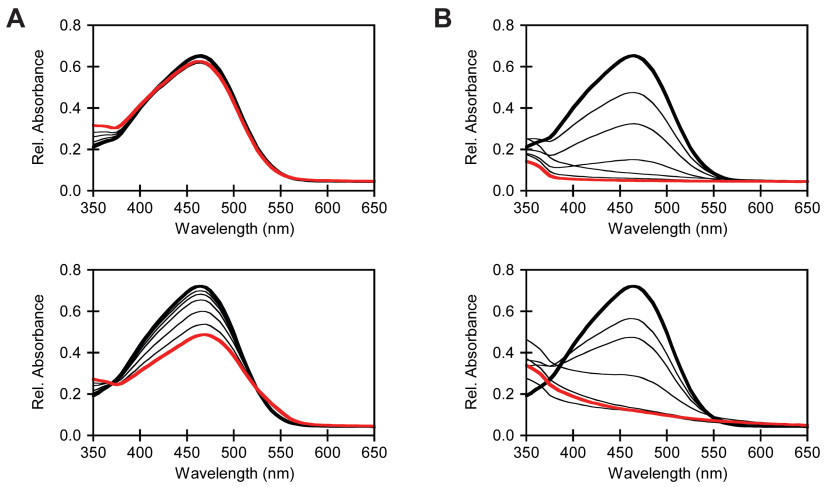

Figure S9. Representative absorbance spectra of methyl orange in the presence of increasing concentrations of (A) Methyl-POP-1 and (B) Urea-POP-1 for two different batches. The POP concentrations range from 0 (black, bold), 0.05, 0.1, 0.2, 0.4, 0.6 and 0.8 (red) mg/mL. All measurements were carried out with 40 μM of methyl orange in ultrapure water (*ca.* pH 7).

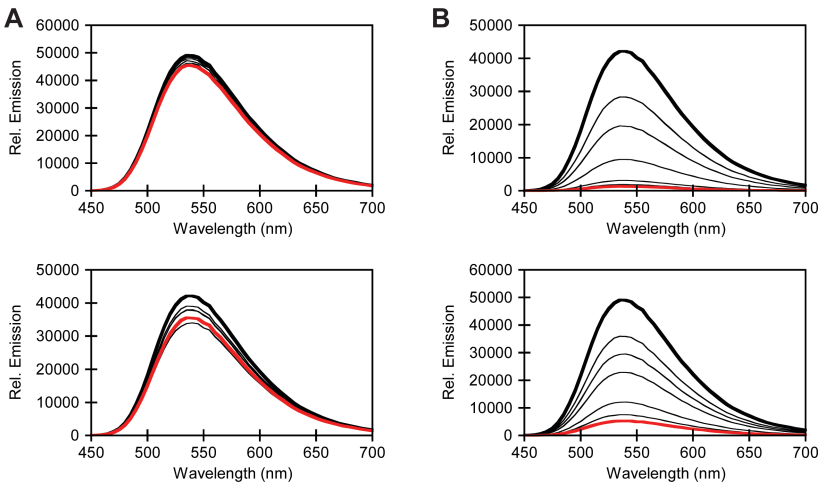

Figure S10. Representative fluorescence spectra of Lucifer Yellow CH in the presence of increasing concentrations of (A) Methyl-POP-1 and (B) Urea-POP-1 for two different batches. The POP concentrations range from 0 (black, bold), 0.05, 0.1, 0.2, 0.4, 0.6 and 0.8 (red) mg/mL. All measurements were carried out with 40 μM of Lucifer Yellow CH in ultrapure water (*ca.* pH 7).

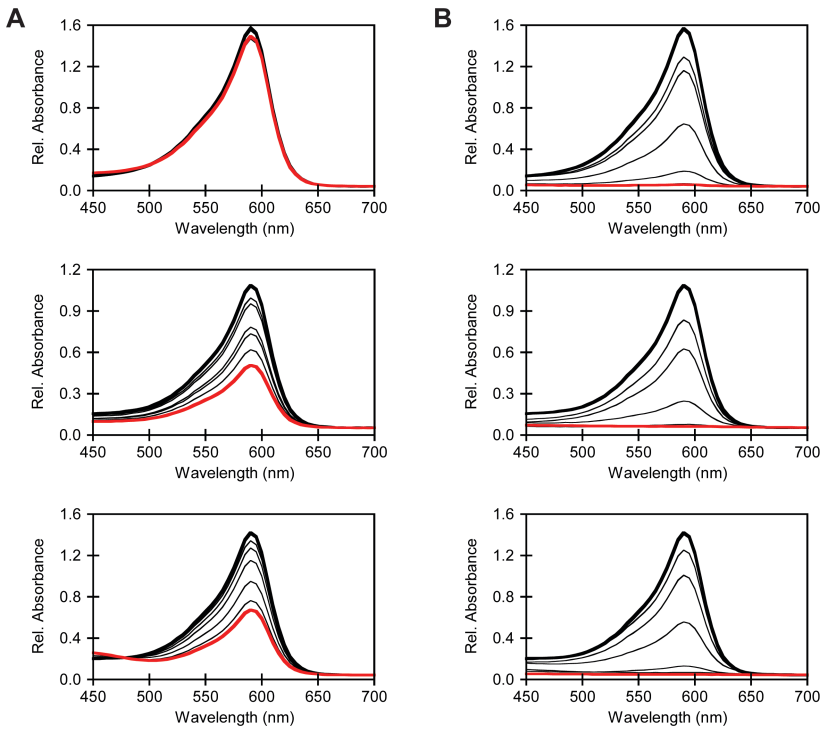

Figure S11. Representative absorbance spectra of bromophenol blue in the presence of increasing concentrations of (A) Methyl-POP-1 and (B) Urea-POP-1 for three different batches. The POP concentrations range from 0 (black, bold), 0.05, 0.1, 0.2, 0.4, 0.6 and 0.8 (red) mg/mL. All measurements were carried out with 40 μM of bromophenol blue in ultrapure water (*ca.* pH 7).

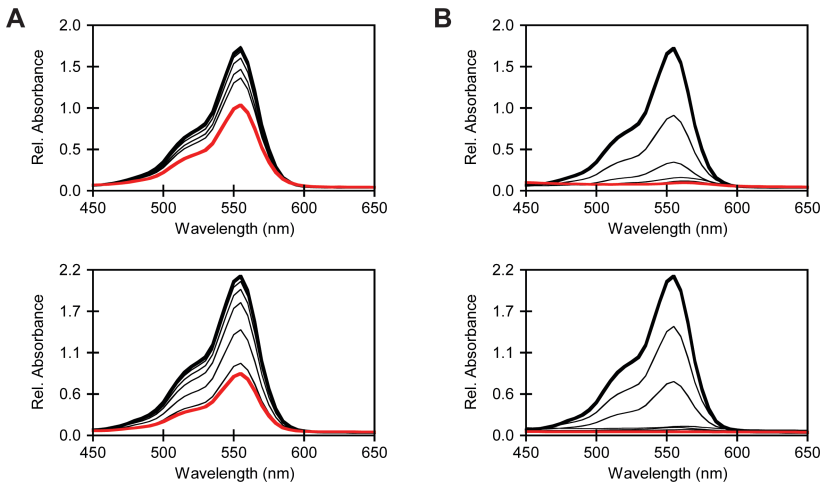

Figure S12. Representative absorbance spectra of Rhodamine B in the presence of increasing concentrations of (A) Methyl-POP-1 and (B) Urea-POP-1 for two different batches. The POP concentrations range from 0 (black, bold), 0.05, 0.1, 0.2, 0.4, 0.6 and 0.8 (red) mg/mL. All measurements were carried out with 40 μM of Rhodamine B in ultrapure water (*ca.* pH 7).

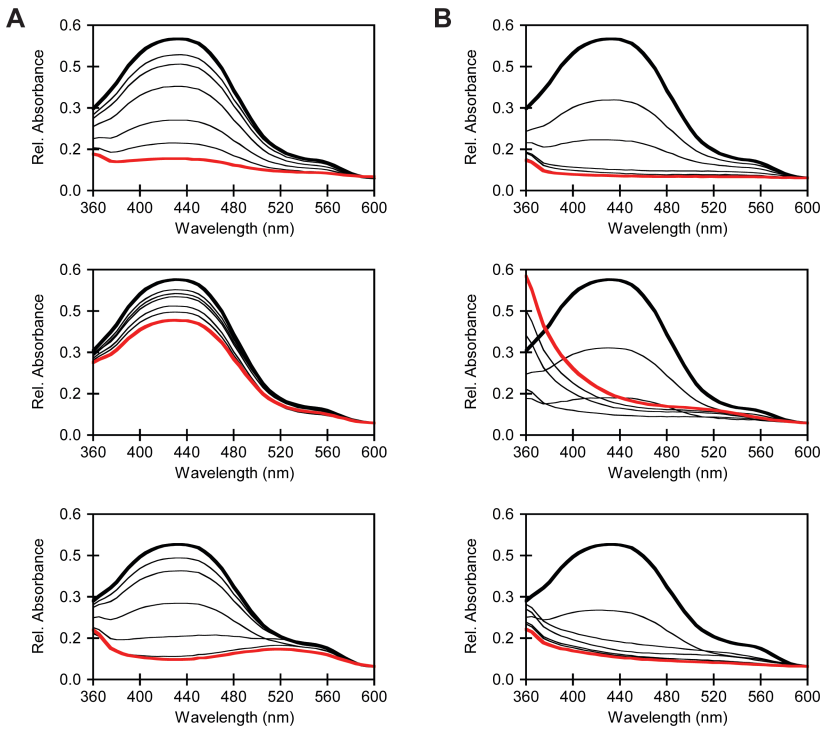

Figure S13. Representative absorbance spectra of methyl red in the presence of increasing concentrations of (A) Methyl-POP-1 and (B) Urea-POP-1 for two different batches. The POP concentrations range from 0 (black, bold), 0.05, 0.1, 0.2, 0.4, 0.6 and 0.8 (red) mg/mL. All measurements were carried out with 40 μM of methyl red in ultrapure water (*ca.* pH 7).

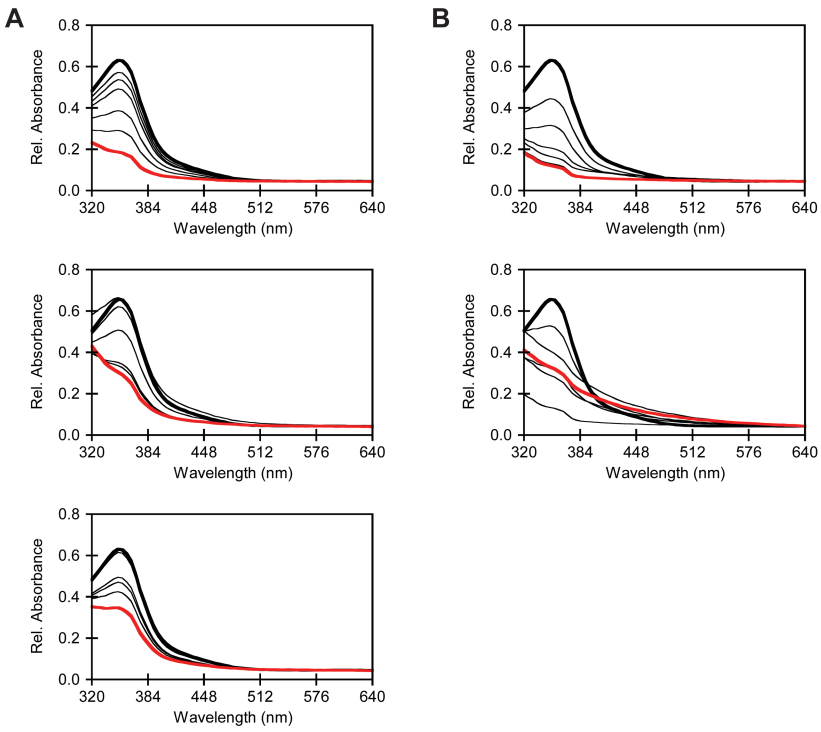

Figure S14. Representative absorbance spectra of Alizarin Yellow G in the presence of increasing concentrations of (A) Methyl-POP-1 and (B) Urea-POP-1 for at least two different batches. The POP concentrations range from 0 (black, bold), 0.05, 0.1, 0.2, 0.4, 0.6 and 0.8 (red) mg/mL. All measurements were carried out with 40 μM of Alizarin Yellow G in ultrapure water (*ca.* pH 7).

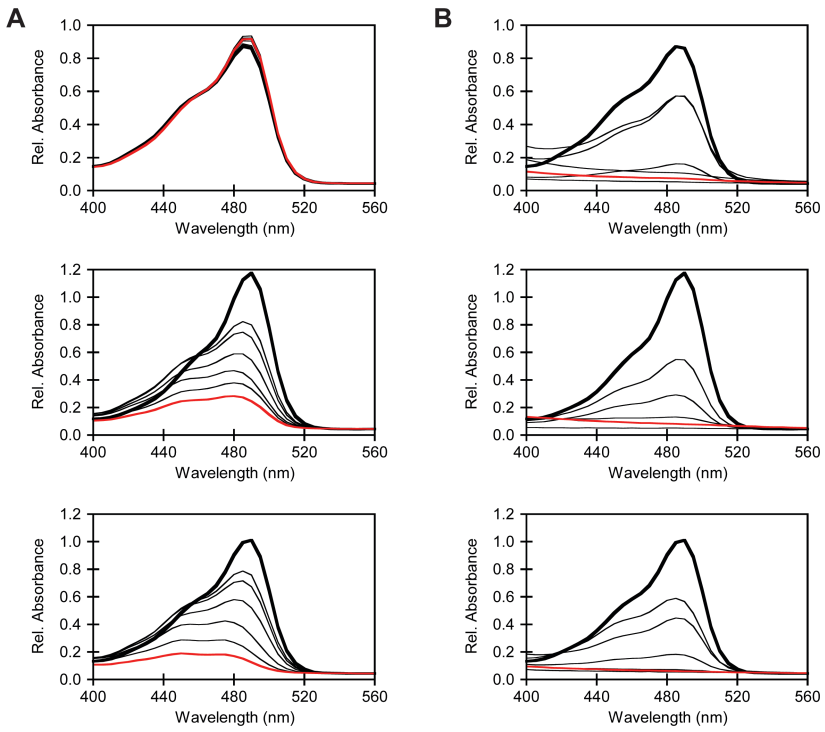

Figure S15. Absorbance spectra of fluorescein in the presence of increasing concentrations of (A) Methyl-POP-1 and (B) Urea-POP-1 for three different batches. The POP concentrations range from 0 (black, bold), 0.05, 0.1, 0.2, 0.4, 0.6 and 0.8 (red) mg/mL. All measurements were carried out with 40 μM of fluorescein in ultrapure water (*ca.* pH 7).

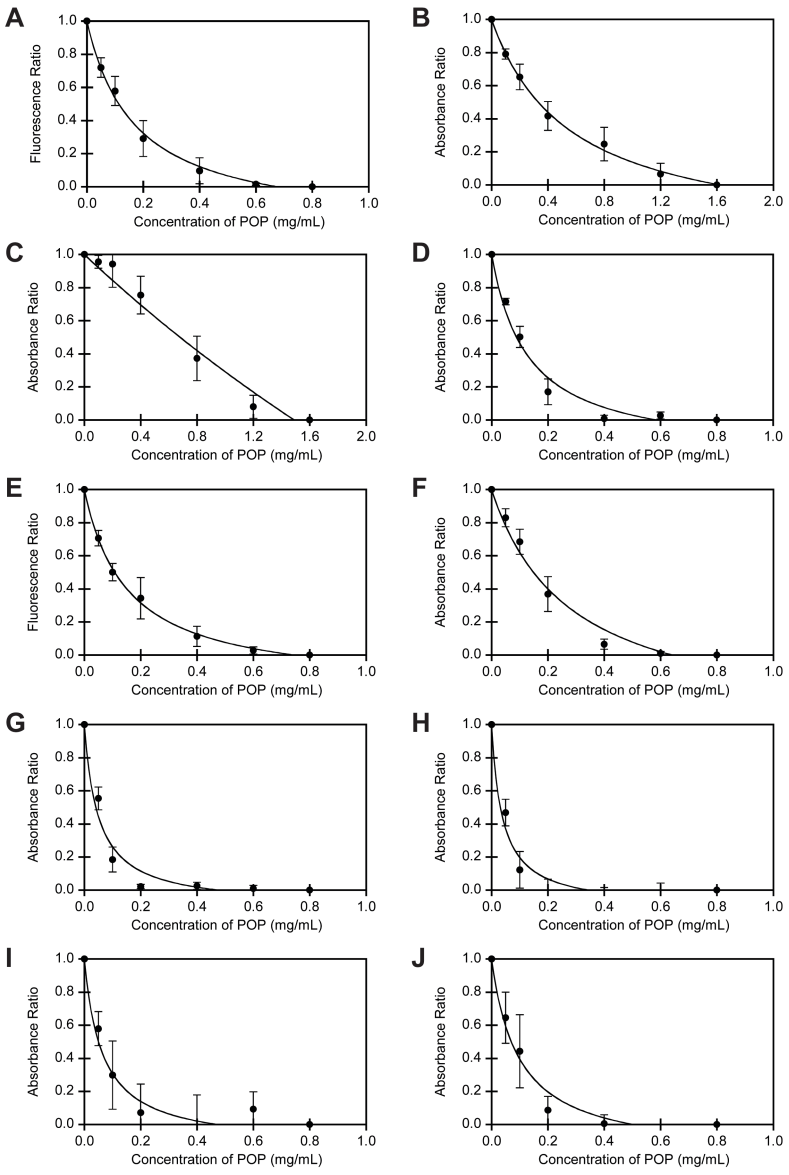

Figure S16. Average curve fit generated from the data in Figure 3 to determine the amount of Urea-POP-1 at the 95% saturation point for (A) flavin mononucleotide, (B) adenosine monophosphate, (C) adenosine triphosphate, (D) methyl orange, (E) Lucifer Yellow CH, (F) bromophenol blue, (G) Rhodamine B, (H) methyl red, (I) Alizarin Yellow G, and (J) fluorescein. The average of at least three technical replicates with standard deviation from at least two different batches of Urea-POP-1 is reported.

Table S3. Summary of the overall charge, partition coefficient, and concentration of Urea-POP-1 at the 95% saturation point for each dye.

Dye	Overall charge at pH 7	Partition coefficient (log *D*)	POP concentration at 95% adsorption saturation (mg/mL)
FMN[a]	-2	-1.4 ± 0.1	1.1 ± 0.2
AMP[a]	-2	-1.5 ± 0.4	1.4 ± 0.2
ATP[a]	-4	-1.08 ± 0.03	N/D
Methyl orange	-1	-1.14 ± 0.03	0.45 ± 0.03
Lucifer Yellow CH	-2	-1.4 ± 0.1	0.56 ± 0.09
Bromophenol blue	-2	-1.6 ± 0.1	0.54 ± 0.05
Rhodamine B	0	1.88 ± 0.04	0.30 ± 0.05
Methyl red	-1	0.46 ± 0.03	0.24 ± 0.08
Alizarin Yellow G	-1	-0.22 ± 0.06	0.4 ± 0.2
Fluorescein	-2	0.21 ± 0.06	0.4 ± 0.1

[a] Abbreviations: Flavin mononucleotide (FMN), adenosine monophosphate (AMP), adenosine triphosphate (ATP)

References

(1) M. R. Golder, C. E. Colwell, B. M. Wong, L. N. Zakharov, J. Zhen and R. Jasti, *J. Am. Chem. Soc.*, 2016, **138**, 6577–6582.
(2) A. M. Fracaroli, H. Furukawa, M. Suzuki, M. Dodd, S. Okajima, F. Gándara, J. A. Reimer and O. M. Yaghi, *J. Am. Chem. Soc.*, 2014, **136**, 8863–8866.
(3) H. Akbulut, T. Endo, S. Yamada and Y. Yagci, *J. Polym. Sci. Part A: Polym. Chem.*, 2015, **53**, 1785–1793.
(4) J. B. Ernst, N. E. S. Tay, N. T. Jui and S. L. Buchwald, *Org. Lett.*, 2014, **16**, 3844–3846.
(5) M. I. Mangione, R. A. Spanevello and M. B. Anzardi, *RSC Adv.*, 2017, **7**, 47681–47688.
(6) Z. Chen, M. Chen, Y. Yu and L. Wu, *Chem. Commun.*, 2017, **53**, 1989–1992.
(7) Y. Oba and S. R. Poulson, *Geochem. J.*, 2012, **46**, 517–520.